



CBAS Global Data Products for Sustainable Development (2022)





International Research Center of Big Data for Sustainable Development Goals

September 2022




CBAS Global Data Products for Sustainable Development (2022)



CONTENTS

Global 30-m spatial distribution of cropland in 2020 (GCL30_2020)	04	
Global 30-m cropping intensity in 2020 (GCI30_2020)	08	
Global 30-m spatial distribution of mangroves in 2000-2020 (GMF30_2000-2020)	12	 

support
SDGs

Global 30-m burned area distribution in 2020 (GBA30_2020)	16	
Global 30-m spatial distribution of forest cover in 2020 (GFC30_2020)	20	
Global 30-m impervious-surface dynamic dataset in 2000-2020 (GISD30_2000-2020)	24	

support
SDGs

Global 30-m spatial distribution of cropland in 2020 (GCL30_2020)

Product summary



The cropland definition was adopted from the Joint Experiment of Crop Assessment and Monitoring (JECAM) network, which defines the annual cropland from a remote sensing perspective as a piece of land of a minimum 0.25 ha meters that is sowed/planted and harvested at least once within the 12 months after the sowing/planting date (Waldner et al., 2016). Considering that cropland might be fallow in a single year, the dataset will use the remote sensing data of three consecutive years (2019-2021) to detect cropland, and in turn ensure its proper classification. A field will be considered as cropland when it is detected as cropland at least once over the three-year period.



"Global 30-m spatial distribution of cropland in 2020" was generated using all available Landsat series and Sentinel-2 satellite imageries during 2019-2021. Due to the difference in crop calendar in the northern and southern hemispheres, there are minor variations in the acquisition dates of remote sensing data used in different agro-ecological zones. Most regions of the northern hemisphere used data from February 2, 2019 to February 1, 2022, while data in many regions in the southern hemisphere were generated using remote sensing data from November 1, 2018 to October 31, 2021. Cropland maps in a few regions were extracted based on satellite imageries from late August 2018 to mid-August 2021 due to unique crop phenology.



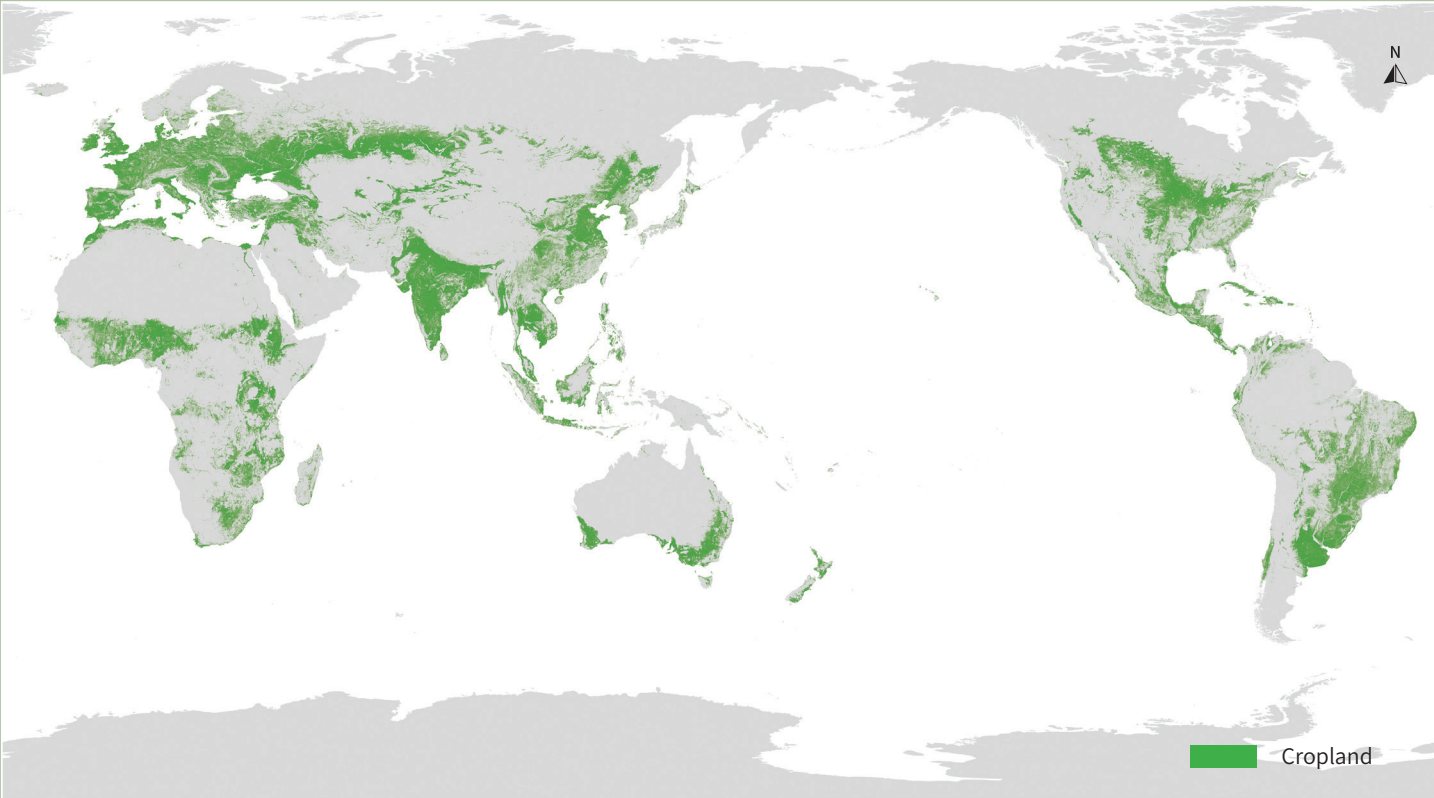
The geographical scope of "Global 30-m spatial distribution of cropland in 2020" covers 180° W to 180° E and 60° S to 80° N. The high latitudes of the northern and southern hemispheres and areas without arable cropland are not within the monitoring scope.

support
SDGs



SDG 2.3.1 Volume of production per labour unit by classes of farming/pastoral/forestry enterprise size.
SDG 2.4.1 Proportion of agricultural area under productive and sustainable agriculture.

Global 30-m spatial distribution of cropland in 2020



Methodology

Cropland data layers from existing datasets were first collected and investigated. Those datasets include Global Food Security Support Analysis Data at 30-m resolution (GFSAD30), Finer Resolution Observation and Monitoring of Global Land Cover (FROM-GLC), Global maps of cropland extent from the University of Maryland, as well as national land cover maps such as ChinaCover, Crop Data Layer for US, Agriculture and Agri-food Canada (AAFC) Annual Crop Inventory (ACI), MapBiomass for Brazil and National crop map for Argentina, etc. Based on independent validation samples, multi-source cropland datasets were integrated into a criteria of higher accuracy and higher spatial resolution (Nabil et al., 2021). For regions with high uncertainty, crowd-sourced in situ measurement, massive remote sensing data and artificial intelligence classifiers were integrated to reproduce the cropland map for each of the corresponding agroecological zones (Bofana et al., 2020). Based on the optimized cropland dataset, Big Earth Data techniques were applied to all available Gaofen-1 imageries in China and Landsat & Sentinel-2 imageries at global scale from 2019 to 2021 to identify cultivated and uncultivated cropland on an annual basis from 2019 to 2021. Annual cultivated cropland maps were composited to generate a global cropland dataset for the three continuous years at 30-m resolution.

Accuracy assessment



Accuracy was first assessed over eight regions with each covering an area of 10°×10° with different agricultural practices. The overall accuracy of the extracted cropland is 90.5% over the eight regions. The assessment was further expanded to global scale, showing the overall accuracy of global high-resolution cropland in 2020 at 89.4%.

Product details

The "Global 30-m spatial distribution of cropland in 2020" was tiled into separate files in GEOTIFF format via GCS_WGS_1984 projection. Globally, 293 tiles were kept where at least one cropland pixel was identified. Each file covers an area of 10° ×10° named in the following format 'Cropland_30m_2019_2021_ \$regions\$.tif'. The file name of each region is defined as "N" or "S" (North Hemisphere or South Hemisphere) followed by two digits of latitude in the top-left corner of the file and "E" or "W" (Eastern Hemisphere or Western Hemisphere) followed by three digits of longitude in the top-left corner. The valid values are 0 and 1, representing non-cropland and cropland, respectively.

Scientific Results:

As shown in GCL30_2020, Asia has the largest cropland area in the world, accounting for about 36.5% of the total, followed by Europe, Africa, North America, South America, and Oceania descending in order. The top eight countries of cropland area are the United States, China, India, Russia, Canada, Brazil, Australia and Argentina, which account for over 50.03% of the world's total cropland. China and India have made great achievements in the conservation and sustainable use of cropland through the construction of irrigation canals and other agriculture infrastructures.

Citation and disclaimer for data use

Users of this product shall clearly indicate the source as "Global 30-m spatial distribution of cropland in 2020 (GCL30_2020)" in the research output, including published or unpublished papers, thesis, reports, dataset and other academic output. Data producers are not responsible for any losses caused by the use of the data. The boundaries and marks used in the maps do not represent any official endorsement or opinion by the data producer.

Dataset citations:

Miao Zhang, Bingfang Wu. Global 30-m spatial distribution of cropland in 2020 (GCL30_2020), Beijing: International Research Center of Big Data for Sustainable Development Goals (CBAS), 2022. doi: 10.12237/casearth.62ff4caa819aec75a535cbe6

References:

Waldner, F., De Abelleira, D., Verón, S.R., et al. (2016). Towards a set of agrosystem-specific cropland mapping methods to address the global cropland diversity. International Journal of Remote Sensing, 37(14), 3196-3231.

Nabil, M., Miao Zhang, Bingfang Wu, et al. (2021). Constructing a 30m African Cropland Layer for 2016 by Integrating Multiple Remote sensing, crowdsourced, and Auxiliary Datasets. Big Earth Data, 1-23.

Bofana, J., Miao Zhang, Nabil, M., et al. (2020). Comparison of different cropland classification methods under diversified agroecological conditions in the Zambezi River Basin. Remote Sensing, 12(13), 2096.



Product URL
https://data.casearth.cn/thematic/cbas_2022

Contact information
Miao Zhang, miaozhang@cbas.ac.cn
Bingfang Wu, bfwu@cbas.ac.cn

Global 30-m cropping intensity in 2020 (GCI30_2020)

Product summary



The cropping intensity, defined as the number of crop cycles during a year, is an important indicator to measure the degree of intensification of cropland utilization. Accurate cropping intensity map could help support the planning of agricultural policies in the future.



" Global 30-m cropping intensity in 2020" was generated using all available Landsat series and Sentinel-2 satellite imageries during 2019-2021. Due to the difference in crop calendar in the northern and southern hemispheres, there are minor variations in the acquisition dates of remote sensing data used in different agro-ecological zones. Most regions used data from February 2, 2019 to February 1, 2022 while products in many regions in the southern hemisphere were generated using remote sensing data from November 1, 2018 to October 31, 2021. Cropping intensity in a few regions was extracted based on satellite imageries from late August 2018 to mid-August 2021 due to the unique crop phenology.



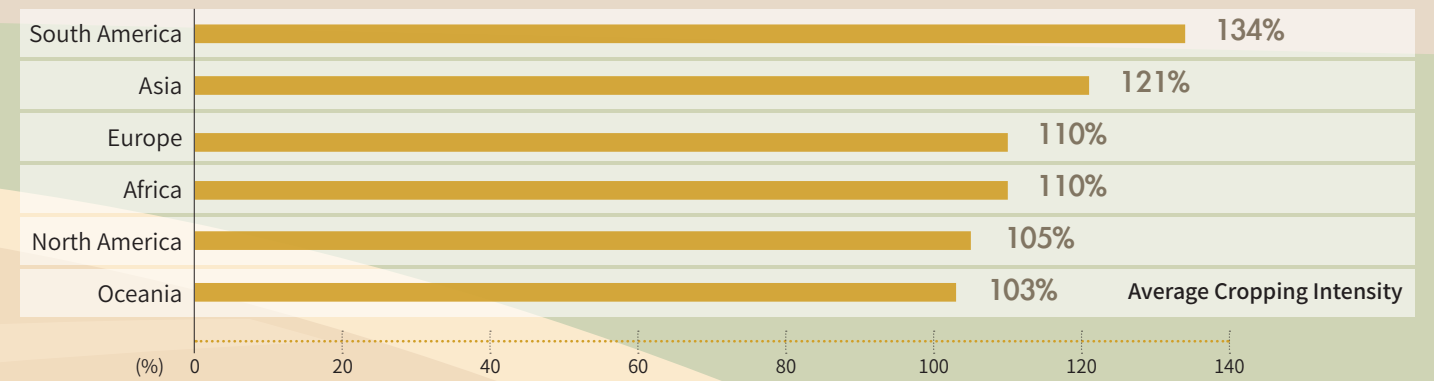
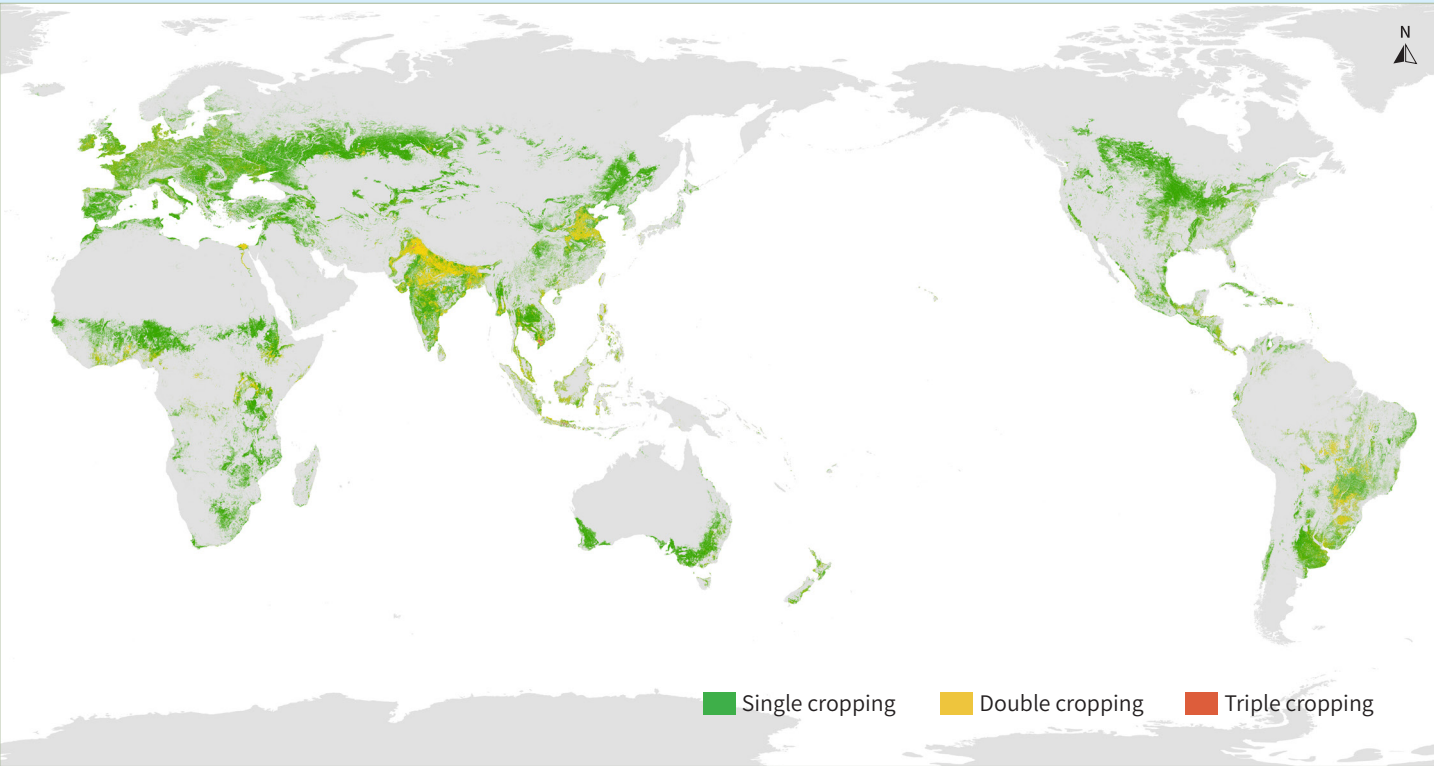
The geographical scope of " Global 30-m cropping intensity in 2020" includes 180° W to 180° E and 60° S to 80° N. High latitude areas in the northern and southern hemispheres and areas with no cropland are not included in the monitoring scope.

support
SDGs



SDG 2.4.1 Proportion of agricultural area under productive and sustainable agriculture.

Global spatial distribution of cropping intensity in 2020



Methodology

Based on all available Landsat, Sentinel and GF 1 imageries from 2019 to 2021, the Normalized Difference Vegetation Index (NDVI) was calculated and integrated into a time series data. Whittaker smoother was then adopted to fill in the areas lacking imageries to reconstruct the NDVI time series. Using this dataset and the full-cycle signal identification method: sow-grow-harvest (Liu et al., 2020; Zhang et al., 2021), the 30-m MCI was calculated. Combining the above process and "Global 30-m spatial distribution of cropland in 2020", this data product was thereby developed.

Accuracy assessment

The whole processing chain was automatically done by online code. All products were quality controlled by the experts to make sure all the tiles were correctly generated. Accuracy was first assessed over eight regions covering an area of 10°×10° across the globe with different agricultural practices. The overall accuracy is 90.4%. The assessment was further expanded to global scale using 3,662 samples, showing an overall accuracy of 92.9% for the whole globe.



Product details

The "Global 30-m cropping intensity in 2020" was tiled into separate files in GEOTIFF format via GCS_WGS_1984 projection. Globally, 293 tiles were kept where at least one cropland pixel exists. Each file covers an area of 10° × 10° named in the following format 'Cropping_Intensity_30m_2019_2021_ \$regions\$.tif'. The "region" in the file name is defined as N/S (North Hemisphere or South Hemisphere) followed by two digits of latitude in the top-left corner of the file and E/W (Eastern Hemisphere or Western Hemisphere) followed by three digits of longitude in the top-left corner. Each file contains two layers in the data product. Values in layer 1 are integers indicating the planting frequency of cropland in 2019-2021. The valid value should be within 100 and the value 100 denotes the background pixel. Values in layer 2 are integers indicating the planting frequency of cropland in 2020. Values 1, 2, and 3 stand for cropping patterns for single-season, double-season, and multi-season respectively. Value 100 in layer 2 denotes the background pixel.

Scientific Results:

Globally, 85.2% of cropland is in single-season cropping pattern, 14.4% in double-season cropping pattern, and only 0.4% in triple-season cropping pattern or above. Cropland in multiple cropping pattern is mainly concentrated in East Asia, Southeast Asia, South Asia, and South America, and over 75% of triple-season cropping pattern is located in tropical regions (5°S to 5°N). The cropping intensity varies widely across continents, ranking from high to low in South America (134%), Asia (121%), Africa (110%), Europe (110%), North America (105%), and Oceania (103%).

Citation and disclaimer for data use

Users of this product shall clearly indicate the source as "Global 30-m cropping intensity in 2020 (GCI30_2020)" in the research output, including published or unpublished papers, thesis, reports, data products and other results. Data producers are not responsible for any losses as a result of the use of this data. The boundaries and markings used for the maps do not imply a formal endorsement or opinion by the data producer.

Dataset citations:

Miao Zhang, Bingfang Wu. Global 30-m cropping intensity in 2020 (GCI30_2020), Beijing: International Research Center of Big Data for Sustainable Development Goals (CBAS), 2022. doi: 10.12237/casearth.62ff4caa819aec75a535cbe7

References:

- Jinlong Fan, Bingfang Wu. (2004). A Methodology for Retrieving Cropping Index from NDVI Profile. Journal of Remote Sensing, 8(6), 628-636. (in Chinese).
- Chong Liu, Qi Zhang, Shiqi Tao, et al. (2020). A new framework to map fine resolution cropping intensity across the globe: Algorithm, validation, and implication. Remote Sensing of Environment, 251, 112095.
- Miao Zhang, Bingfang Wu, Hongwei Zeng, et al. (2021). GCI30: a global dataset of 30 m cropping intensity using multisource remote sensing imagery. Earth System Science Data, 13(10), 4799-4817.



QR code

Product URL
https://data.casearth.cn/thematic/cbas_2022

Contact information
Miao Zhang, miaozhang@cbas.ac.cn
Bingfang Wu, bfwu@cbas.ac.cn

Global 30-m spatial distribution of mangroves in 2000-2020 (GMF30_2000-2020)

Product summary



Mangrove forests are swampy, woody plant communities mainly composed of evergreen shrubs or trees distributed in the coastal wetlands of tropical and subtropical regions throughout the world. The wetland ecosystem has important ecological, economic, and landscape values in the coastal zone.



The product was generated using multi-temporal Landsat series satellite images with no clouds or less than 20% cloud cover, including four periods of 2000, 2010, 2015 and 2020.



180° W–180° E,
35° S–35° N

support
SDGs

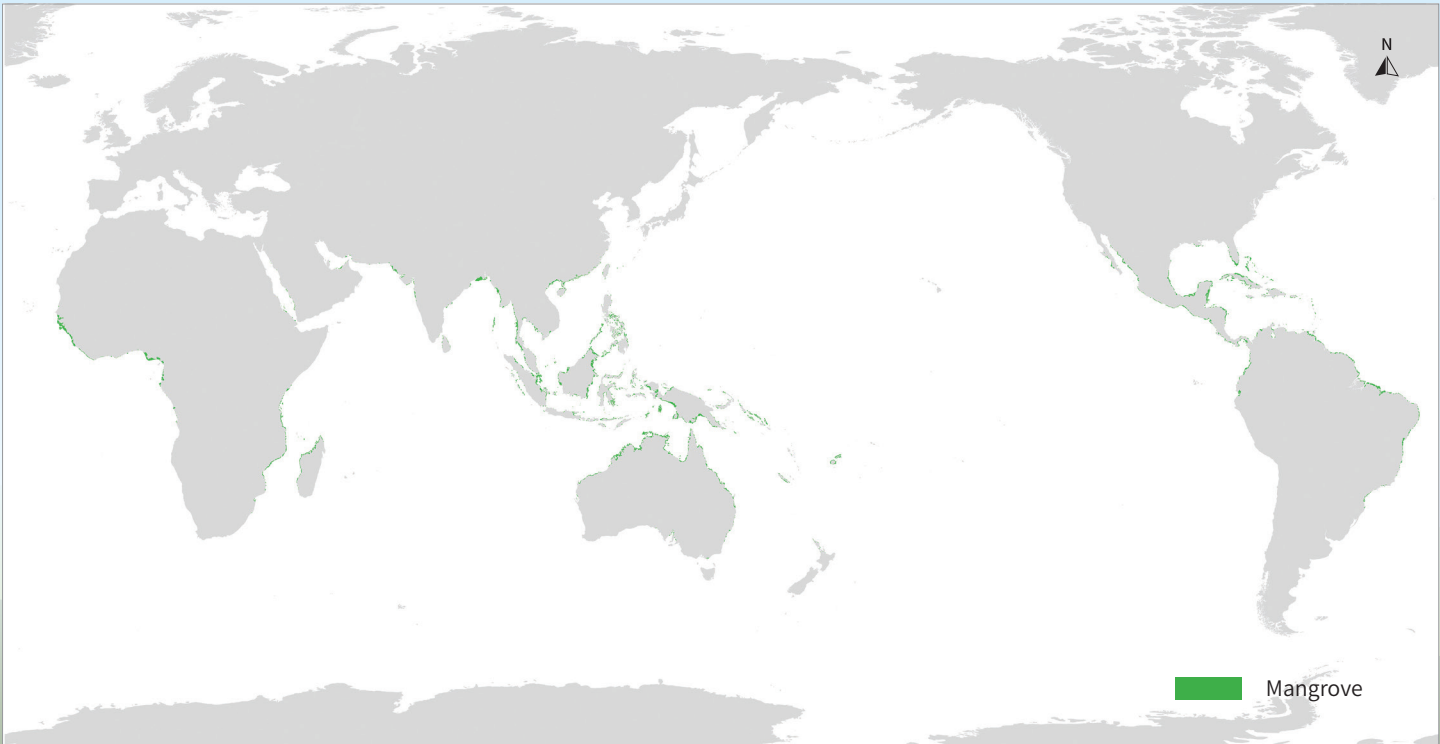


SDG 6.6.1 Change in the extent of water-related ecosystems over time.

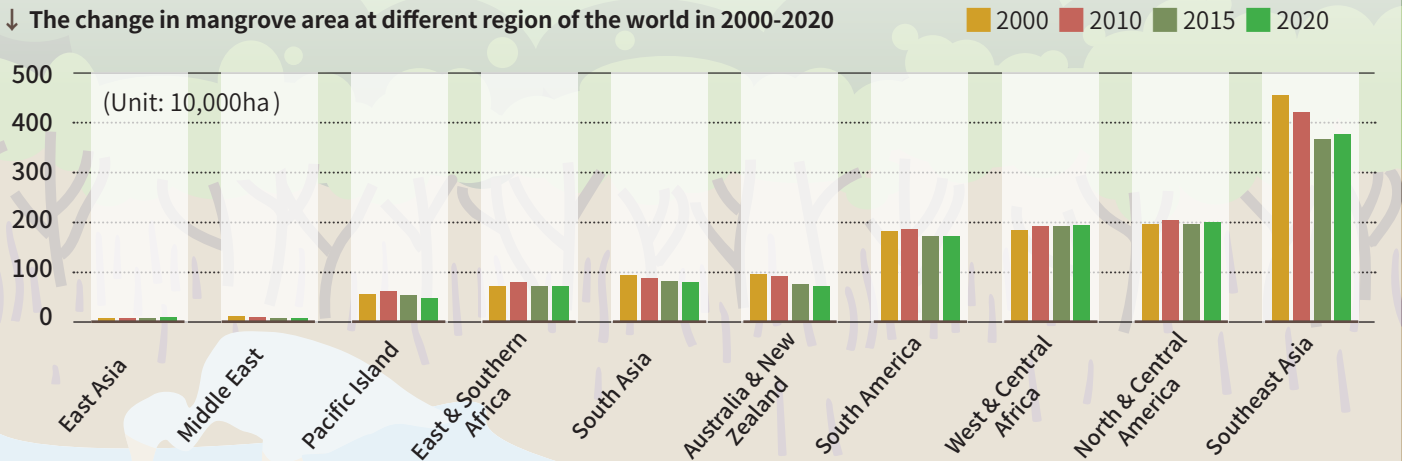


SDG 14.2 Sustainably manage and protect marine and coastal ecosystems to avoid significant adverse impacts.

Global spatial distribution of mangroves in 2020



The change in mangrove area at different region of the world in 2000-2020



Methodology

Four periods of global mangrove distribution datasets in 2000, 2010,2015 and 2020 were generated by mapping the global mangrove change with a combination of the Capsules-Unet deep learning model (Guo et al., 2021a; 2021b) and visual interpretation of imagery using multi-temporal Landsat images with no clouds or less than 20% cloud cover after pre-processing such as atmospheric correction and band combination.

Accuracy assessment



Overlapping areas from publicly available mangrove datasets (including the Mangrove Forests Map of the World (WMF) and the Global Mangrove Watch (GMF)) were used as the reference areas for selecting mangrove validation samples. These validation samples were randomly deployed in the relevant global areas by referencing high-resolution images in the same year. 2,489 validation points were deployed, including 1,443 mangrove points and 1,046 non-mangrove points. The overall accuracy (OA), user accuracy (UA), product accuracy (PA) and Kappa coefficient calculated using the error matrix method, as well as the F1-score for comprehensive measure of classification accuracy, were used to evaluate the mangrove extraction accuracy, and the overall accuracy of mangrove extraction is greater than 88%. The Kappa coefficient and F1-score are greater than 0.76 and 0.88, respectively.

Product details

The datasets adopted the WGS84 coordinate system, latitude and longitude projection (EPSG: 4326), and Shapefile format for coordination, projection and storage respectively.

Scientific Results:

During 2000-2010, mangrove forests in Asia, the Middle East, Australia and New Zealand all showed a decreasing trend, while in Africa, North and South America, and the Pacific Islands increased slightly. From 2010-2015, the global regions are generally decreasing to varying degrees, except for East Asia, where there is a significant increase. From 2015-2020, East Asia, Southeast Asia and Africa show a small increase, while other regions still show a decreasing trend.

From the changes of mangroves in different periods, it can be seen that the global trend of mangrove decline has gradually slowed down since 2000 as people's awareness of mangrove protection has increased, especially in East Asia, such as China, where the growth trend of mangroves is more obvious due to the government's policy of returning ponds to forests and wetlands, as well as the projects of mangrove restoration and protection.



Citation and Disclaimer for Data Use

Users of this product shall clearly indicate the source as " Global 30-m spatial distribution of mangroves in 2000-2020 (GMF30_2000-2020)" in all forms of research output, including, but not limited to, published and unpublished papers, theses, manuscripts, books, reports, data products, and other academic output. The data producers are not responsible for any losses caused by the use of the data. The boundaries and marks used in the maps do not represent any official endorsement by or opinion of the data producers.

Dataset citations:

Jingjuan Liao. Global 30-m spatial distribution of mangroves in 2000-2020 (GMF30_2000-2020), Beijing: International Research Center of Big Data for Sustainable Development Goals (CBAS), 2022. doi: 10.12237/casearth.62ff4caa819aec75a535cbe8

References:

Yujuan Guo, Jingjuan Liao, Guozhuang Shen. A deep learning model with Capsules embedded for high-resolution image classification, IEEE Journal of Selected Topics in Applied Earth Observations and Remote Sensing, 2021a, 14, 214-223.

Yujuan Guo, Jingjuan Liao, Guozhuang Shen. Mapping large-scale mangroves along the Maritime Silk Road from 1990 to 2015 using a novel deep learning model and Landsat data. Remote Sens. 2021b, 13, 245.



Product URL
https://data.casearth.cn/thematic/cbas_2022

Contact information
Jingjuan Liao, jjliao@cbas.ac.cn

Global 30-m burned area distribution in 2020 (GBA30_2020)

Product summary



Burned area refers to the land area where vegetation has been burned by fire, including forest burned area, grassland burned area and farmland burned area. The 2020 burned area products include all burned area that occurred in that year.



"Global 30-m burned area distribution in 2020" was generated with all available Landsat 7/8 satellite data acquired from January 1 to December 31, 2020, i.e., full time series Landsat 7/8 satellite data.

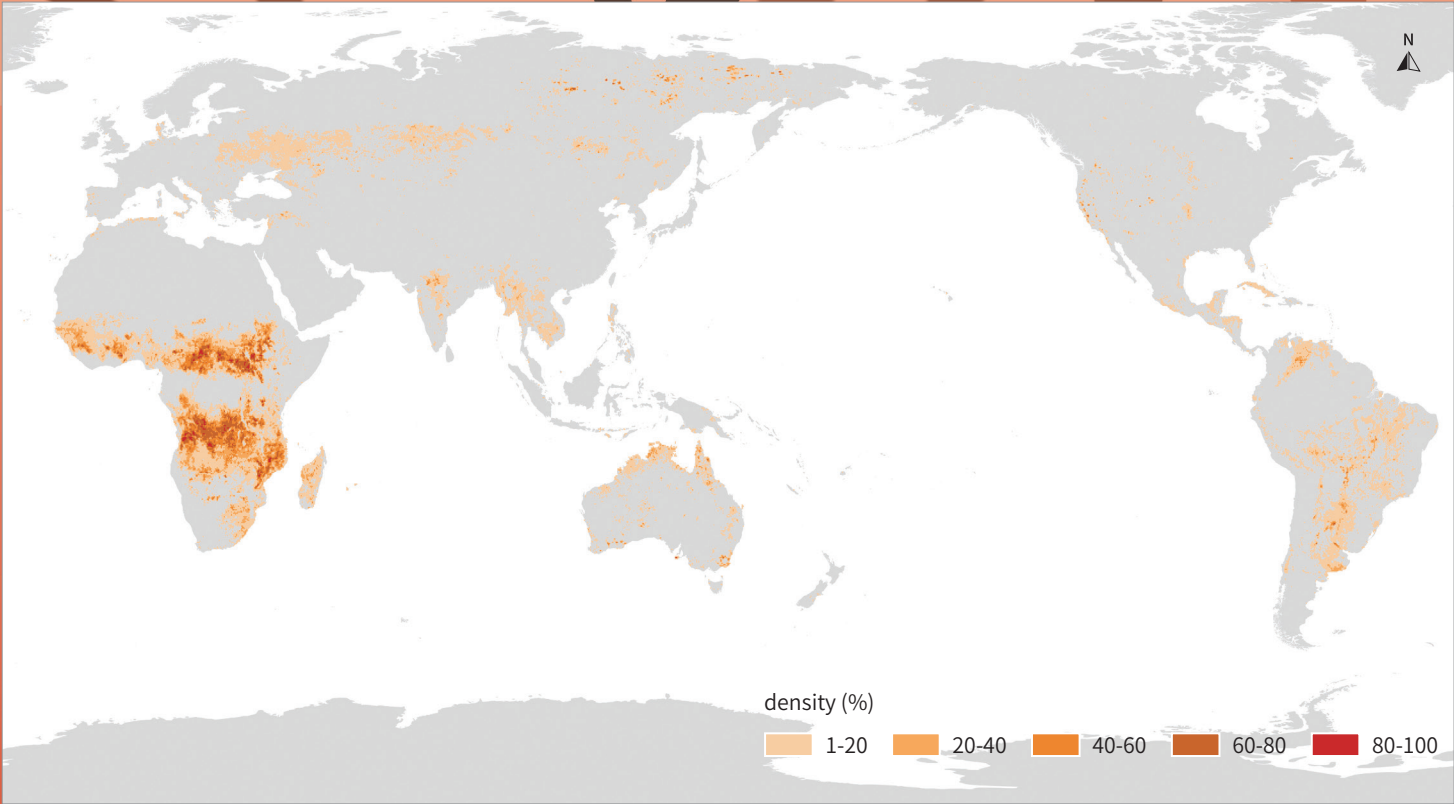
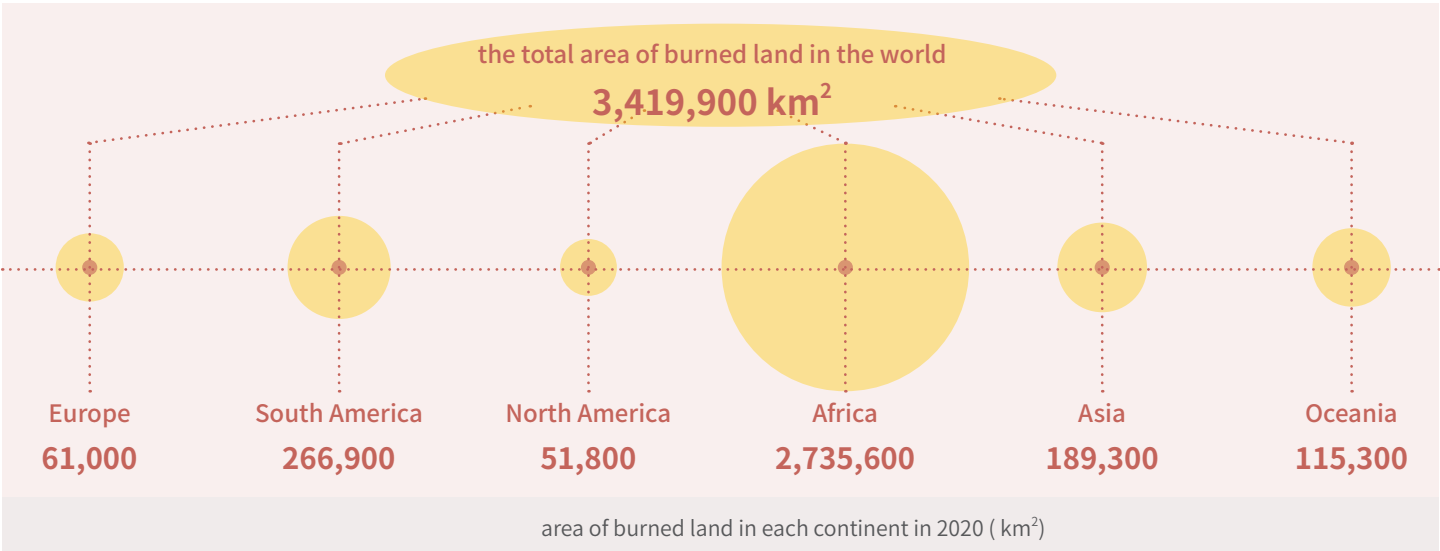


180° W-180° E,
60° S-80° N

support
SDGs



SDG 13.1 Strengthen resilience and adaptive capacity to climate-related hazards and natural disasters in all countries.



Spatial distribution of global burned area density (percentage of burned pixels in every 0.25°×0.25° grid) in 2020

Methodology

Based on time series Landsat 7/8 images and high-quality sample database, the "Global 30-m burned area distribution in 2020" product was generated using multi-source burned area sensitive parameters and the random forest algorithm.

According to the characteristics of global ecosystem distribution and fire behavior, burned and unburned samples were selected in different regions of the world. Samples of burned areas include burned areas of different types, with different burned degrees and recovery periods. Samples of unburned areas contain various land cover types, including vegetation, water, bare land, especially the cover types that are easy to be confused with burned area, such as topographic shadows, built up area, and so on.

Using multi-source sensitive parameters for burned area extraction (band surface reflectance, NBR, NBR2, BAI, MIRBI, etc.), the random forest algorithm is employed for sample training and learning to get the recognition rules and seed points of the burned land, and the regional growth method is carried out to obtain the spatial distribution of burned areas.

Accuracy assessment



Multiple data sources were used in the accuracy validation, including Landsat 7/8, GF 1, and MTBS (Monitoring Trends in Burn Severity) products. By collecting the full time series satellite data of the whole year in the verification sample area, burned areas occurring in 2020 were visually identified, and the satellite images before and after the fire were determined. Based on the satellite images, the reference data for burned area products verification were obtained by manual visual interpretation. Validation results show the overall accuracy of the global burned area product is 91.3%.

Product details

The "Global 30-m burned area distribution in 2020" product was projected in a geographic (Lat/Long) projection at 0.00025° (approximately 30 m) with the WGS84 horizontal datum and the EGM96 vertical datum. The results consist of 504 10° × 10° tiles, and each tile contains about 40,000 × 40,000 pixels. The data format is GeoTIFF.

Each tile was coded according to the latitude and longitude in the upper left corner, with latitude in the front and longitude in the back. Latitude is 2 digits, with N/S as prefix; longitude is 3 digits, with E/W as prefix, where N is used at 0° latitude, and E is used at 0° longitude. Each tile file contains a layer, where the value of 1 represents the burned area, and the value of 0 represents the unburned area.

Citation and disclaimer for data use

Users of this product shall clearly indicate the source as "Global 30-m resolution burned area distribution in 2020 (GBA30_2020)" in the research output, including published or unpublished papers, thesis, reports, dataset and other academic output. Data producers are not responsible for any losses caused by the use of the data. The boundaries and marks used in the maps do not represent any official endorsement or opinion by the data producer.

Dataset citations:

Zhaoming Zhang, Guojin He, Tengfei Long, Mingyue Wei. Global 30-m burned area distribution in 2020 (GBA30_2020), Beijing: International Research Center of Big Data for Sustainable Development Goals (CBAS), 2022. doi: 10.12237/casearth.62ff4d13819aec75a535cbea

References:

Tengfei Long, Zhaoming Zhang, Guojin He, et al. 30 m Resolution Global Annual Burned Area Mapping Based on Landsat Images and Google Earth Engine. Remote Sensing, 2019, 11:489-519.
Dongchuan Pu, Zhaoming Zhang, Tengfei Long, et al. Global 30-m burned area product validation using stratified random sampling. Journal of Remote Sensing, 2020, 24(5): 550-558. DOI: 10.11834/jrs.20209171(in Chinese).



Product URL

https://data.casearth.cn/thematic/cbas_2022

Contact information

Zhaoming Zhang, zmzhang@cbas.ac.cn
Guojin He, gjhe@cbas.ac.cn

Scientific Results:

The burned areas are concentrated mainly in central and southern Africa, northern Australia, and central and southern South America. Most of the aforementioned areas are located near the equator, with high temperatures, sufficient fuel, and long dry seasons, as fires are prone to occur in dry seasons. Statistics indicate that in 2020 the total area of burned land in the world was 3,419,900 km². Africa had the largest burned area of 2,735,600 km² in 2020, accounting for 79.99% of the globe.

Global 30-m spatial distribution of forest cover in 2020(GFC30_2020)

Product summary



"Forest" in the "Global 30-m spatial distribution of forest cover in 2020" product refers to land spanning more than 0.5 hectares with trees higher than 5 meters and a canopy cover of more than 10% , or trees able to reach these thresholds in situ. It does not include land that is predominantly under agricultural or urban land use.



The product was generated preferentially from all available data during the peak season of global forest growth in 2020. When optimal timing cannot be met due to cloud cover or data quality, try to select data with a similar time.



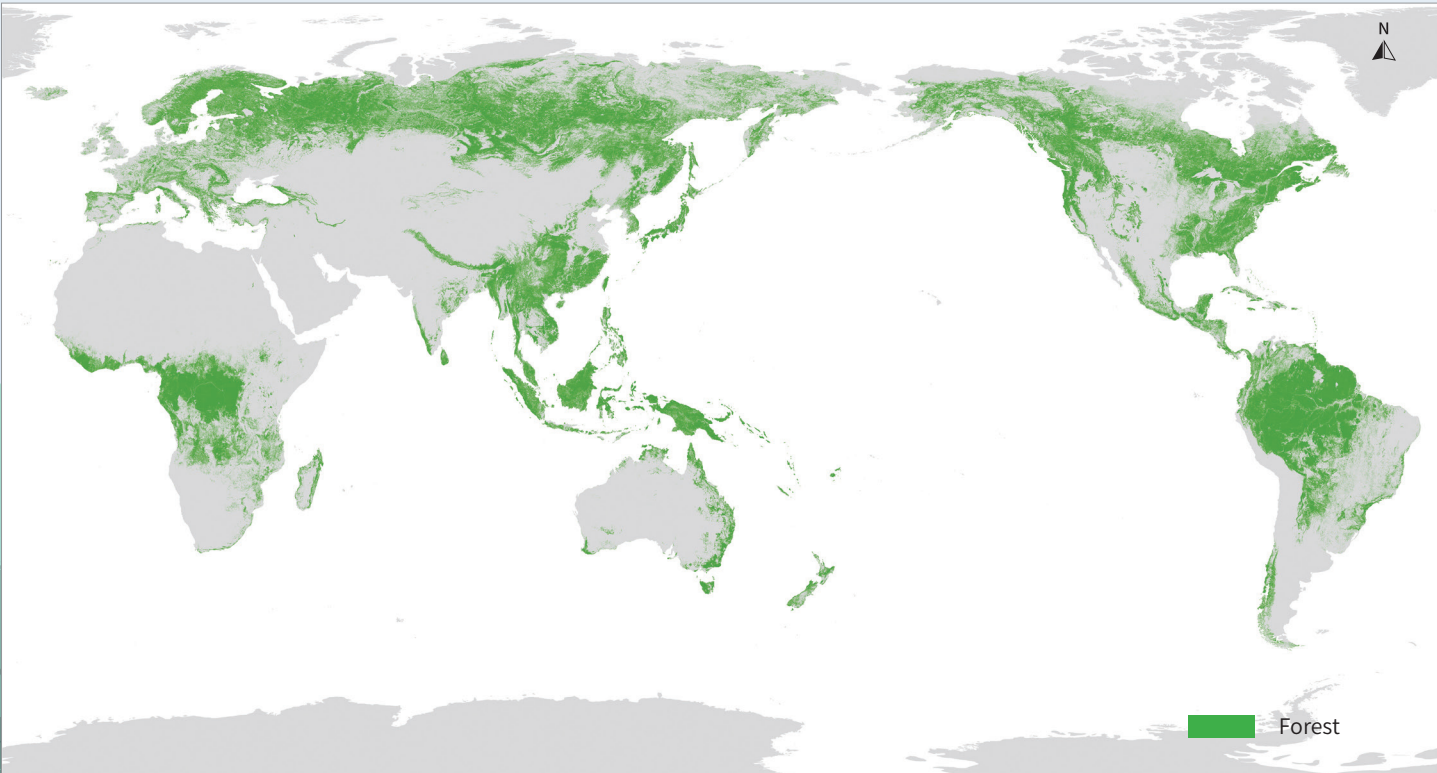
180° W–180° E
60° S–80° N

support
SDGs



SDG 15.1.1, forest area as a proportion of total land area.

Global 30-m map of forest cover in 2020



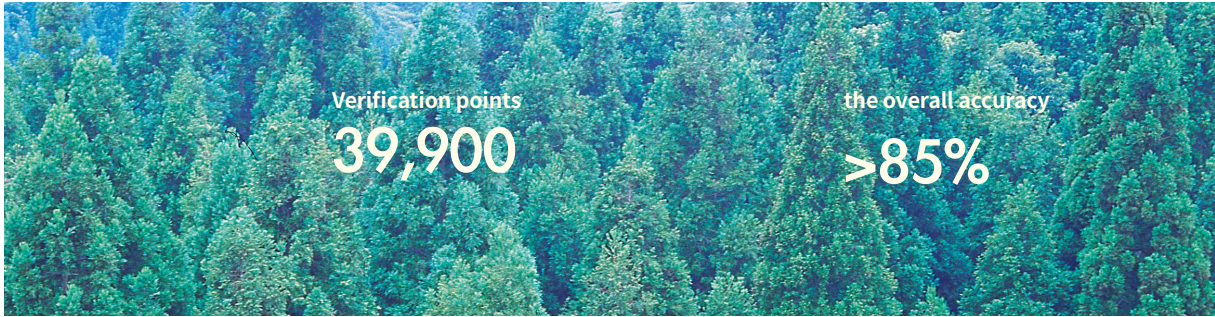
Method and data resources

The data sources of the product were acquired from the Landsat series, GF-1, and GF-6 satellites, and the product was generated based on global ecosystem partitions, multi-source sample data, and machine learning algorithms (Zhang et al., 2020).

Referring to the FAO Global Ecological Zones (GEZ) (FAO, 2000) map, the world was divided into different forest cover zones. Taking into account both spatial continuity and moderate size, the regions with good consistency of forest cover types and non-forest cover types were divided together. Finally, the global land was divided into 43 regions with consistent forest and non-forest characteristics.

The stratified random sampling method was used to obtain samples from multi-source data such as global flux sites and the global forest sample plot data of the Global Forest Dynamics Monitoring Network, and a total of 61,653 sample points were obtained. High-resolution satellite images such as GF-1, GF-2, GF-6 and QuickBird were used for validation.

Accuracy assessment



High-resolution satellite images such as GF and other related data products, combined with part of the field survey data, were used as reference data. A total of 39,900 validation points were collected. The accuracy verification results showed that the overall accuracy of global forest cover products reached over 85%.

Product details

The product was projected in a geographic (Lat/Long) projection at 0.00025° (approximately 30-m resolution), with the WGS84 horizontal datum and the EPSG:4326 vertical datum. The results consist of 504 tiles of 10°×10°, and each tile contains about 40,000×40,000 pixels. The data format is GeoTIFF.

Each tile is coded according to the latitude and longitude shown in the upper left corner, with latitude in the front and longitude in the back. Latitude is two digits, with a prefix of N/S; longitude is three digits, with a prefix of E/W, where N is used at 0° latitude, and E is used at 0° longitude. Each tile file contains a layer in which the value of 1 represents forest and the value of 0 represents non-forest area.

Scientific Results:

By the end of 2020, the total forest area in the world was 3.684 billion hectares, accounting for 28.03% of the total global land area, equivalent to 0.47 hectares per person.

The spatial distribution of global forests is uneven, with obvious distinctions from different climate zones. "Tropical forest" covers the largest area, accounting for almost half (47.40%) of the total global forest area, with the forest coverage of 29.54%. Although the forest area of the north frigid zone is only about a quarter of the world, the forest coverage is the highest, reaching 52.89%.

There are significant differences in the distribution of forests across the six continents (excluding Antarctica). Asia has the largest land area and the largest forest area, ranking fourth in the world in terms of forest coverage. Although the forest area of South America ranks second in the world, it has the highest forest coverage at 43.6%, which is related to the distribution of large areas of tropical rainforest in the Amazon Basin. The forest area of North America accounts for 19.78% of the globe, with a forest coverage of 32.68%.

Citation and disclaimer for data use

Users of this product shall clearly indicate the source as "Global 30-m spatial distribution of forest cover in 2020" in all forms of research output, including, but not limited to, published and unpublished papers, theses, manuscripts, books, reports, data products, and other academic output. The data producers are not responsible for any losses caused by the use of the data. The boundaries and marks used in the maps do not represent any official endorsement by or opinion of the data producers.

Dataset citations:

Xiaomei Zhang, Guojin He, Tengfei Long, et al. Global 30-m spatial distribution of forest cover in 2020 (GFC30_2020), Beijing: International Research Center of Big Data for Sustainable Development Goals (CBAS), 2022. doi: 10.12237/casearth.625e1760819aec2a46dcd2d8

References:

Xiaomei Zhang, Tengfei Long, Guojin He, et al. Rapid generation of global forest cover map using Landsat based on the forest ecological zones[J]. Journal of Applied Remote Sensing, 2020, 14(2):1.



Product URL

https://data.casearth.cn/thematic/cbas_2022

Contact information

Xiaomei Zhang, xmzhang@cbas.ac.cn

Global 30-m impervious-surface dynamic dataset in 2000-2020 (GISD30_2000-2020)

Product summary



The impervious-surface area is defined as a land cover where surface water is unable to penetrate the ground due to the presence of anthropogenic materials, such as steel, cement, asphalt, bricks, and stone, leading to blockage of the natural evapotranspiration process.



GISD30 dataset includes five global 30-m impervious-surface maps, i.e., 2000, 2005, 2010, 2015 and 2020.



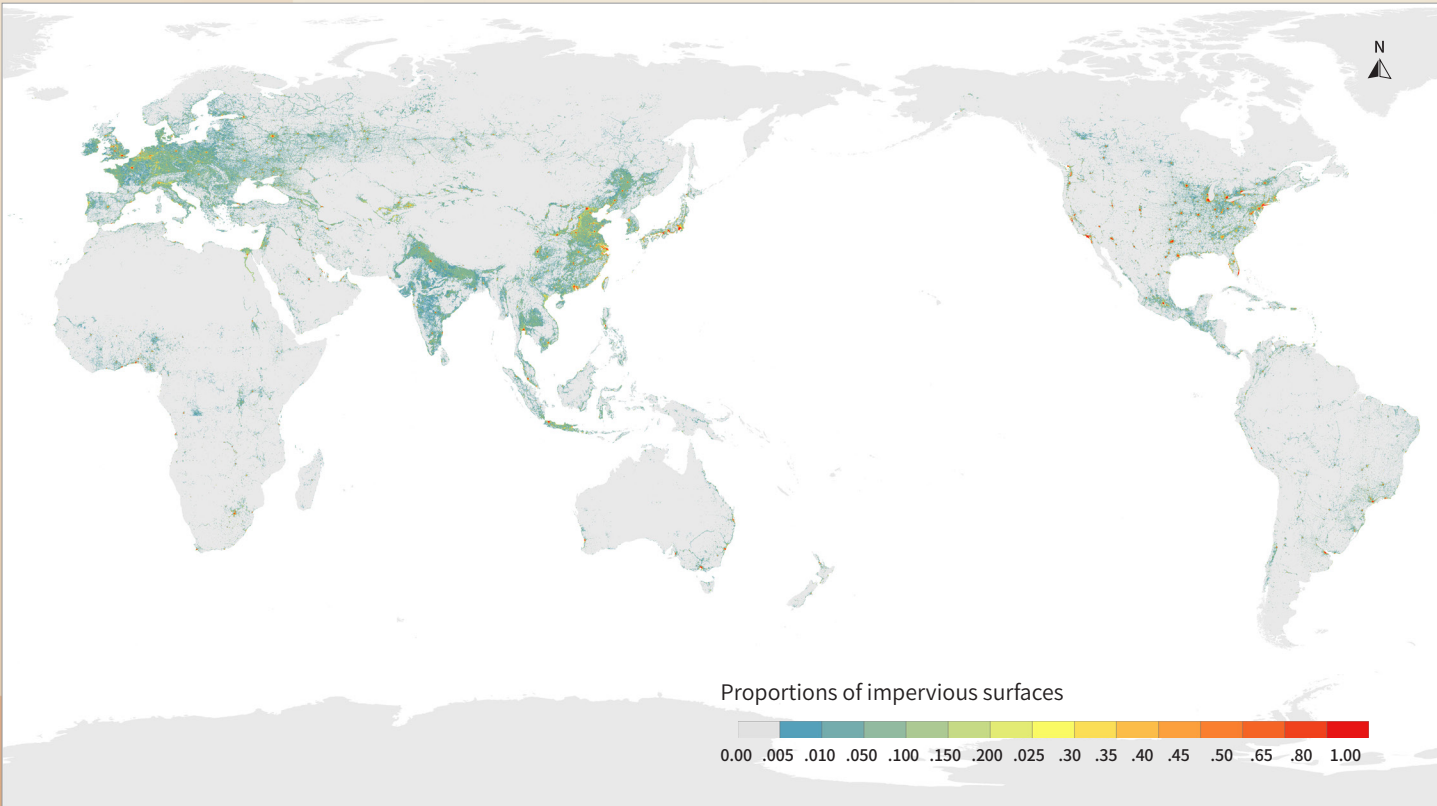
180° W–180° E
60° S–80° N

support
SDGs



SDG 11.3, sustainable urbanization.

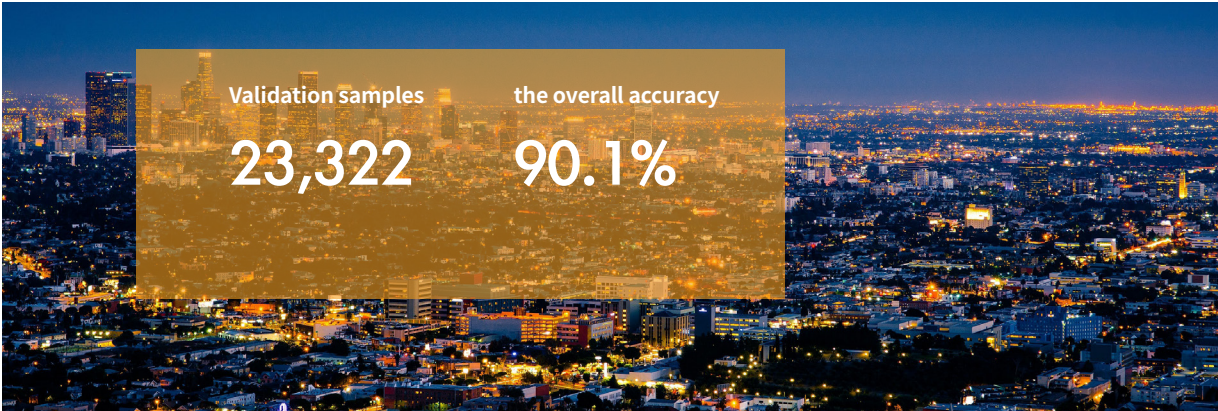
Global 30-m map of impervious-surface in 2020



Methodology

To produce GISD30, a high confidence training dataset at global scale was collected by utilizing a prior land cover data according to a series of extraction rules. The spectral generalization approach and a sample migration strategy were designed to achieve long-term dynamic monitoring of impervious surfaces. The GISD30 dataset was ultimately produced by classifying the time-series Landsat reflectance imagery and integrating the local adaptive random forest model and the spectral generalization approach (Zhang et al. 2021, 2022).

Accuracy assessment



The stratified random sampling strategy was utilized to assess accuracy. A total of 23,322 time-series validation samples were collected based on the visual interpretation method. The validation results show that the GISD30 dataset achieved an overall accuracy of 90.1% and a kappa coefficient of 0.865, which is significantly higher than similar products both in China and internationally.

Product details

The product is stored using the WGS84 coordinate system (EPSG: 4326) with a spatial resolution of 30-meter. The output format is GeoTIFF. Each tiled file covers a 5°×5° geographical grid corresponding to 18,554×18,554 pixels. The dataset contains a total of 961 tiled files.

For accurate usage and reference, the GISD30 files are named in the following format: GISD30_1985-2020_E/W***N/S***.tif

where 'E/W***N/S***'is the longitude and latitude coordinates found in the upper left corner of the tile data. Each tiled file contains a single-layer map that showcases the surface status with 0 and 1, representing pervious surfaces and impervious surfaces, respectively.

Scientific Results:

GISD30 revealed a significant increase in impervious-surface area at the global scale. It increased from 696,000 km² in 2000 to 1,107,300 km² in 2020, with an increase of 411,300 km² (59.08%). The expansion of impervious surface exhibits significant geographical and spatial distribution features, with Asia showing the largest growth at 207,600 km², followed by North America, Europe, Africa, South America, and Oceania. The global impervious surface expansion area is mainly located in the regions between 20° N and 60° N, in accordance with the latitudinal distribution.

Citation and disclaimer for data use

Users of this product shall clearly indicate the source of the data as "Global 30-m impervious-surface dynamic dataset in 2000-2020 (GISD30_2000-2020)" in all forms of research output, including, but not limited to, published and unpublished papers, theses, manuscripts, books, reports, data products, and other academic output. The data producers are not responsible for any losses caused by the use of the data. The boundaries and marks used in the maps do not represent any official endorsement by or opinion of the data producers.

Dataset citations:

Liangyun Liu, Xiao Zhang. Global 30-m impervious-surface dynamic dataset in 2000-2020 (GISD30_2000-2020), Beijing: International Research Center of Big Data for Sustainable Development Goals (CBAS), 2022. doi: 10.12237/casearth.625e14c1819aec2a46dcc033

References:

Xiao Zhang, Liangyun Liu, Xidong Chen, et al. Automatically Monitoring Impervious Surfaces Using Spectral Generalization and Time Series Landsat Imagery from 1985 to 2020 in the Yangtze River Delta. Journal of Remote Sensing, 2021, 1-16, <https://doi.org/10.34133/2021/9873816>.

Xiao Zhang, Liangyun Liu, Tingting Zhao, et al. GISD30: global 30-m impervious surface dynamic dataset from 1985 to 2020 using time-series Landsat imagery on the Google Earth Engine platform. Earth System Science Data, 2022, 14, 1831–1856, <https://doi.org/10.5194/essd-2021-285>.



Product URL
https://data.casearth.cn/thematic/cbas_2022

Contact information
Liangyun Liu, lyliu@cbas.ac.cn



International Research Center of Big Data for Sustainable Development Goals

Address: No. 9 Dengzhuang South Road, Haidian District, Beijing

Postal code: 100094

Telephone: +86 10 82177601

E-mail: datasharing@cbas.ac.cn

Map Approval Number: GS (2022) 1928